

University of Nebraska - Lincoln

DigitalCommons@University of Nebraska - Lincoln

Papers in Natural Resources

Natural Resources, School of

2015

An Anomaly-Based Method for Identifying Signals of Spring and Autumn Low-Temperature Events in the Yangtze River Valley, China

Weihong Qian

Yun Cheng

Man Jiang

Qi Hu

Follow this and additional works at: <https://digitalcommons.unl.edu/natrespapers>



Part of the [Natural Resources and Conservation Commons](#), [Natural Resources Management and Policy Commons](#), and the [Other Environmental Sciences Commons](#)

This Article is brought to you for free and open access by the Natural Resources, School of at DigitalCommons@University of Nebraska - Lincoln. It has been accepted for inclusion in Papers in Natural Resources by an authorized administrator of DigitalCommons@University of Nebraska - Lincoln.

An Anomaly-Based Method for Identifying Signals of Spring and Autumn Low-Temperature Events in the Yangtze River Valley, China

WEIHONG QIAN AND YUN CHEN

Department of Atmospheric and Oceanic Sciences, Peking University, Beijing, China

MAN JIANG

Department of Atmospheric and Oceanic Sciences, Peking University, Beijing, and Shanghai Central Meteorological Observatory, Shanghai, China

QI HU

School of Natural Resources and Department of Earth and Atmospheric Sciences, University of Nebraska—Lincoln, Lincoln, Nebraska

(Manuscript received 17 September 2014, in final form 11 February 2015)

ABSTRACT

Abnormally low temperature (LT) events in spring and autumn can cause severe damage to spring and autumn rice production in the mid- to lower Yangtze River valley in China. Advanced predictions of such events can help mitigate their damage. However, the current methods have limited success in describing and predicting those weather events. In this study, a new method is proposed to decompose any one of the meteorological variables into its climatic component and an anomaly, and the anomaly is used in identifying signals of the LT events. The method is used in 20 strong spring LT events and 44 autumn events during 1960–2008. The results show the advanced ability of this method to clearly describe the LT events as compared with the vague indications of such events that are produced by conventional methods currently in practice in China. In addition, the composite profile of vertical anomalies shows that a negative center of geopotential height anomalies at around 300 hPa, coexisting with a strong cold center of temperature anomalies at 850 hPa, is a signature for LT events. For the 44 autumn LT events and 20 spring LT events during 1960–2008, their early disturbances were identified up to 10.2 days and 6.9 days, respectively, before the occurrence of the LT events in the valley. This result suggests that identifying the early disturbances and extracting anomalous signals from the products of current medium-range weather forecast models may be a potential way to improve the prediction skill for LT events in the valley.

1. Introduction

One of the high-impact weather events adversely affecting agriculture in the mid- to lower Yangtze River valley in China is the anomalously low temperatures (LT) that persist in the valley for 3 or more days during spring or autumn. The climate in southern China allows for double- or even triple-cropping systems for rice each year. Early April is when the spring rice crop is planted. The crop grows to maturity and is harvested in July.

Following the harvest, the autumn rice crop is planted in early August and harvested in middle October. Persistent LT events for prolonged periods in April and May can severely damage sprouting in rice growth, leading to replanting or loss of crops. Similarly, prolonged LT events in late September and early October will stop the flowering and kernel filling and ruin the autumn rice production. In spring, such events over a prolonged period of unseasonably cold temperature are associated with cold surges that interrupt the climatic (or normal) spring warming process. They are often referred to as the returning cold. In autumn, similar abnormal events, which occur when cold air dips south bringing strong and cold winds, are called cold dew winds, because of the accompanying strong cold wind during the events. These

Corresponding author address: Weihong Qian, Dept. of Atmospheric and Oceanic Sciences, Peking University, Beijing 100871, China.

E-mail: qianwh@pku.edu.cn

meteorological events have been recognized, defined, and documented at the China Meteorological Administration (State Standardization Committee 2012). They have been examined and studied over the years in an effort to provide warnings to farmers who may apply mitigation strategies to reduce the impacts of such events on their rice production (e.g., Du 2005; Wang et al. 2009; Chen et al. 2013).

In their attempts at predicting the spring or autumn LT events in the mid- to lower Yangtze River valley, forecasters have been relying on analyzing the numerical weather predictions made by the major operational centers, such as the European Centre for Medium-Range Weather Forecasts (ECMWF) and the National Centers for Environmental Prediction (NCEP) with its Global Forecast System (GFS). These centers provide predictions of atmospheric circulation patterns and conditions at a lead time of 1–2 weeks.

However, the forecasting performances of these models remain problematic for extreme temperature events, such as heat waves and cold events, with lead times of more than 5 days. For example, a recent comparison of three global numerical weather prediction (NWP) models (the T639 model of the China National Meteorological Center, the ECMWF global model, and a global spectral model developed by the Japan Meteorological Agency) showed that although the ECMWF model performed the best among the three for a major heat wave event that occurred in the lower Yangtze River valley during the summer of 2013, its predictions for the event's duration, areal coverage, and transition time were not skillful beyond 5 days (Zhang and Li 2013). For a low-temperature and freezing-rain event that occurred during the winter of 2008 in south China, no correct forecast from these models was made 5 days in advance (Ding et al. 2008). Predictions of extreme LT events in spring are even more difficult to make accurately, and only a few studies of such events have been reported. It is thus necessary and important to explore new strategies and methods for successfully forecasting surface LT events with lead times of 5–10 days. The economic value of such forecasts to rice as well as fruit farmers in south China is enormous.

In this paper, we introduce a new method that uses daily weather analyses to indicate and trace disturbances that could cause LT events in the valley. Because such events are caused by extreme cold surface air temperature anomalies compared to the spring or fall seasonal average, the strategy is to find a connection between the cold surface air temperature anomalies and anomalies of other atmospheric variables, while the latter can be derived from observations and NWP model output. Although anomaly-standardized analyses, which are

suitable for all climate zones, have gradually attracted the attention of forecasters and researchers alike in the last decade (Easterling et al. 2000; Yan and Yang 2000; Grumm and Hart 2001; Hart and Grumm 2001), they have not been applied to forecasting the extreme cold events during the crop-growing seasons in China. Du et al. (2014) have recently expanded this concept and suggested the use of “ensemble anomaly forecasting,” which makes use of anomaly forecasts that are based on ensembles of NWP forecasts. In that method, the use of ensembles helps to improve the confidence of the anomaly forecast. Similarly, an “extreme forecast index” method has been used at the ECMWF (Lalurette 2003; Zsoter 2006).

In recent years, another method that directly applies anomaly-based variables has been proposed and used in short-, medium-, and extended-range forecasts of many extreme weather events in China, including freezing rain (Qian and Zhang 2012), heat waves (Ding and Qian 2011), and typhoon tracks (Qian et al. 2014). This method was also used in the study of daily regional heavy rain events in eastern China from January to September in 2010. With the aid of this method, the lead time of anomalous convergence signals in the lower troposphere extracted from the forecasting model outputs of the ECMWF was improved to 6.7 days when these heavy rains were indicated (Qian et al. 2013). Qian et al. (2013) suggested that the anomaly-based variables can be extracted from model predictions and processed to identify signals of extreme weather events at a lead time of up to 1 week.

In this paper, we describe the details of the anomaly-based method and show its potential forecast skill for the LT events in the mid- and lower Yangtze River basin. In the next section (section 2), we describe the two datasets and the method used to decompose one of the atmospheric variables into a climatic component and an anomaly. All of the spring and autumn LT events in the basin during the period 1960–2008, based on the criteria defined by the State Standardization Committee in China, are identified and listed in section 3. Results from using the anomaly-based method to diagnose and trace the anomalous early signals of those LT events that occurred in the mid- and lower Yangtze River basin are shown and discussed in section 4. Section 5 contains a summary demonstrating the potential forecasting skill for those severe events.

2. Data and methodologies

a. Data

The NCEP–NCAR reanalysis, with a horizontal 2.5° latitude–longitude grid interval and at the standard pressure levels from 1000 to 50 hPa (Kalnay et al. 1996), is used in this study. In addition, the daily mean,

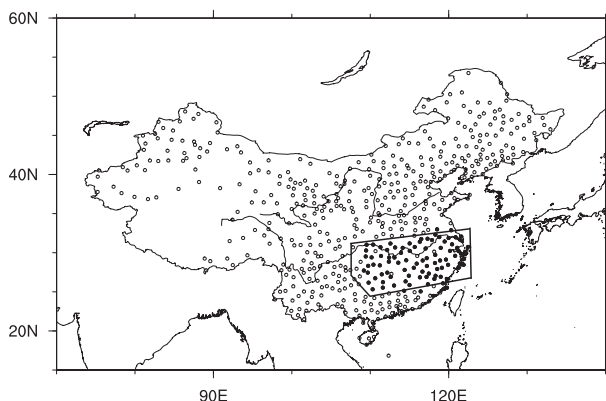


FIG. 1. The 549 surface observation stations across mainland China (open and solid circles). The solid circles mark the 88 stations inside the boxed study domain. Several open circles near the Yangtze River inside the box mark stations in complex terrain and are excluded from this study.

maximum, and minimum surface air temperature observations in mainland China are also used. These data are taken from 549 observational stations across China (Fig. 1) and cover the period from 1960 to 2008 (Li and Yan 2009). Several stations in mountainous areas are excluded from this study because the strong local terrain effects severely limited their representations of temperatures in surrounding areas. Daily (24 h) precipitation observations (from 1200 UTC to the next 1200 UTC) at the same 549 stations are obtained from the China Meteorological Administration. Our study area for the LT events focuses on the Chongqing District, and Hunan, Jiangxi, Hubei, and Zhejiang Provinces, as well as the southern parts of Anhui and Jiangsu Provinces, and the northern part of Fujian Province (the boxed area in Fig. 1). Within this area there are 88 stations among the 549 stations in mainland China.

b. Methodologies

We use an anomaly-based method to examine the LT events and develop a method for diagnosing and tracing their early signals. As was done in our previous studies (Qian et al. 2014), an atmospheric variable $F_{d,y}(\lambda, \varphi, p, t)$ on a calendar day t in year y at a spatial point of pressure level p , longitude λ , and latitude φ can be decomposed into its daily climatic mean $\bar{F}_d(\lambda, \varphi, p, t)$ and its temporal deviation $F'_{d,y}(\lambda, \varphi, p, t)$ from the mean:

$$F_{d,y}(\lambda, \varphi, p, t) = \bar{F}_d(\lambda, \varphi, p, t) + F'_{d,y}(\lambda, \varphi, p, t). \quad (1)$$

In (1), the subscript d indicates the daily mean, which in this case is the 30-yr (1979–2008) average of an observed variable on the calendar day d . For example, when d is set on 1 May, t represents the days of 1 May 1979, 1 May 1980, ..., 1 May 2008 for a total of 30 yr:

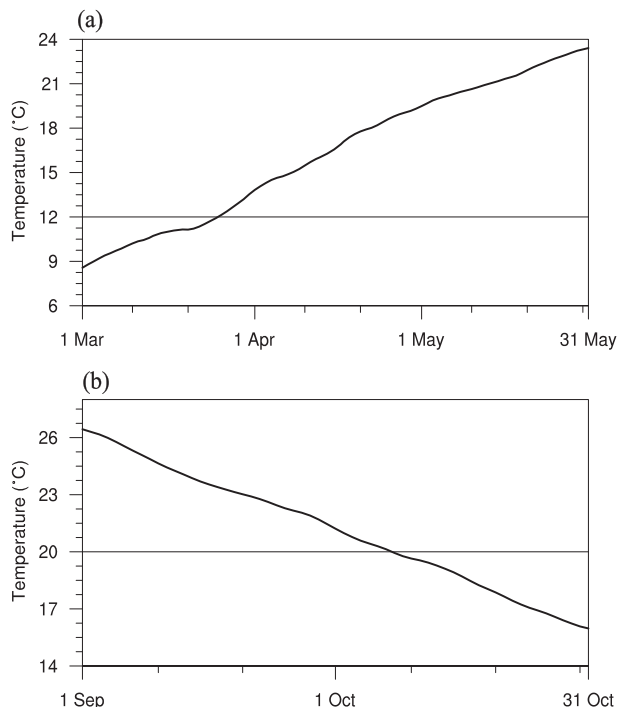


FIG. 2. Climatic daily mean surface air temperature ($^{\circ}\text{C}$) averaged from all 88 stations in the valley during (a) spring (1 Mar–31 May) and (b) autumn (1 Sep–31 Oct).

$$\bar{F}_d(\lambda, \varphi, p, t) = \sum_{y=1979}^{2008} F_{d,y}(\lambda, \varphi, p, t)/30. \quad (2)$$

The climatic mean defined in (2) varies from day to day, depicting a seasonal cycle.

3. Low-temperature events

a. Definitions

April is the vegetative growth season after the spring rice crop is planted in the mid- to lower Yangtze River valley. During this time, the spike differentiation in rice growth will be inhibited if the daily mean surface air temperature is colder than 12°C according to Chen et al. (2013). For the autumn rice crop in the valley, its flowering and filling processes occur in September. During this time, if the daily mean surface air temperature is colder than 20°C , such processes may be terminated, resulting in empty and shriveled grains, and even the loss of the harvest. Because of this critical role of low temperatures during that period, the temperature threshold from 1 September to 10 October of each year has been documented by the China Meteorological Administration for agricultural use (Feng et al. 1985).

To provide a background or reference for the LT events in the two seasons, we show in Fig. 2 the

climatology (1979–2008) of the daily mean surface air temperature averaged from the 88 stations in the valley during spring and autumn. In spring (Fig. 2a), the daily mean surface air temperature starts to exceed 12°C around 26 March. Climatologically, the temperature will smoothly increase from that day onward, and reach 13.8°C on 1 April. Thus, when the daily mean temperature at one station is colder than 12°C in April or May, the area represented by the station has a cold surface with damagingly low temperatures for the spring rice crop. In autumn (Fig. 2b), the daily mean surface air temperature gradually decreases from above to below 20°C on 8 October. When the daily mean temperature at a station is colder than 20°C in late September or early October, the area represented by that station has a cold surface with damagingly low temperatures for the autumn rice crop.

In a previous study (Chen et al. 2013) and government document (Feng et al. 1985), daily mean temperatures colder than 12°C in spring and colder than 20°C in autumn were used as the criteria for LT events. Three criteria in time, space, and intensity were used to determine an LT event by Zhang and Qian (2011). In this study, an LT event is defined as a period of three or more consecutive days (time) over an area with five or more adjacent stations (space) of daily mean temperature colder than 12°C in spring and colder than 20°C in autumn having a negative deviation (intensity) from the climatology over the past 30 years (1979–2008).

Using these data and definitions, the historical autumn LT events have been identified. Furthermore, these LT events are categorized into cold dry events and cold wet events separated by the absence or presence of precipitation during the LT events (State Standardization Committee 2012). The difference between the cold wet and cold dry events is that the former occur when cold air invades the valley from the north and forms a stationary front in the valley with a warmer air mass to its south. Along the stationary or quasi-stationary front, it is rainy under rather low surface temperatures. The latter occurs in the absence of such a stationary front. The weather processes in the cold dry events are primarily strong cold air masses moving from the north to the valley and even to the south China coast. The entire region including the river valley and southern China is under a cold high pressure system. The cold high pressure system brings, in addition to the cold temperature, clear skies and strong northerly surface winds. The clear skies during nocturnal hours enhance surface cooling and create rather low surface temperatures that are particularly harmful to rice crops. Cold dry events often cause more severe cold injuries to rice plants than do cold wet events. That is another reason for the state

TABLE 1. Results for 17 regional dry LT events in autumn. The case highlighted in boldface font is used in vertical and tracing analyses.

Start date	Duration (days)	Coverage (No. of stations)	Intensity (anomaly; °C)	<i>R</i>
2 Oct 1960	8	52	−2.42	0.15
30 Sep 1967	10	82	−6.09	0.27
30 Sep 1969	11	76	−3.88	0.09
29 Sep 1970	10	84	−5.92	0.29
3 Oct 1972	4	69	−2.79	0.25
6 Oct 1973	5	67	−2.48	0.3
4 Oct 1979	7	75	−2.33	0.01
2 Oct 1985	5	60	−4.06	0.17
30 Sep 1986	4	70	−3.67	0.14
26 Sep 1988	3	51	−3.36	0.05
5 Oct 1988	5	67	−1.84	0.3
7 Oct 1989	4	61	−1.79	0.08
5 Oct 1991	6	63	−1.45	0.16
30 Sep 1993	5	58	−2.63	0.23
6 Oct 1993	3	53	−0.83	0.03
6 Oct 2002	5	71	−2	0.11
1 Oct 2004	8	86	−4.93	0.08

standardization in China to separately categorize the cold dry events and the cold wet events.

b. Low-temperature events during 1960–2008

The onset date of a regional LT event in autumn in the valley is defined as the day when more than one-half (≥ 44) of the stations in the valley (Fig. 1) reach their site LT event threshold. A regional cold wet event is distinguished from a regional cold dry event by the ratio of the number of rainy sites N_r to the total number of sites N in the LT event:

$$R = N_r/N. \quad (3)$$

In the study of Zhang et al. (1995), three types of LT event were used: cold dry events with $R \leq 0.3$, cold wet events with $R \geq 0.7$, and hybrid cold events with $0.3 < R < 0.7$. In this study, we categorize the cold events into two groups based on the R values: cold dry events with $R \leq 0.3$ and cold wet events with $R > 0.3$. Using these criteria, we identified 17 regional cold dry events and 27 regional cold wet events from 1 September to 10 October 1960–2008 (Tables 1 and 2). In Table 1, the smallest $R = 0.01$, indicating the driest event, which started on 4 October 1979 and lasted for 7 days. At the opposite extreme, in Table 2, the largest $R = 0.93$, indicating the wettest event, which started on 12 September 1981 and lasted for 3 days. To summarize, there were 7, 11, 11, and 11 (dry and wet) LT events between 1 September and 10 October in the 1960s, 1970s, 1980s, and 1990s, respectively. From 2000 to 2008, there were a total of four regional LT events.

TABLE 2. As in Table 1, but for the 27 regional wet LT events in autumn.

Start date	Duration (days)	Coverage (stations)	Intensity (anomaly; °C)	<i>R</i>
4 Oct 1963	7	68	-2.46	0.47
6 Oct 1964	5	79	-2.31	0.6
6 Oct 1965	5	73	-2.7	0.8
28 Sep 1968	4	65	-3.89	0.31
1 Oct 1971	10	78	-3.47	0.47
23 Sep 1972	3	73	-4.95	0.61
19 Sep 1974	3	63	-5.47	0.76
4 Oct 1974	3	53	-2.66	0.92
8 Oct 1974	3	52	-1.77	0.58
6 Oct 1977	5	78	-3.8	0.39
4 Oct 1978	3	51	-2.22	0.55
22 Sep 1980	4	74	-4.29	0.71
12 Sep 1981	3	61	-5.36	0.93
1 Oct 1981	10	68	-7.14	0.77
27 Sep 1982	3	45	-6.57	0.52
6 Oct 1983	4	63	-1.87	0.55
3 Oct 1984	8	86	-5.43	0.73
4 Oct 1992	7	83	-5.15	0.4
3 Oct 1994	5	64	-2.27	0.64
3 Oct 1995	8	79	-3.61	0.61
6 Oct 1996	5	84	-6	0.79
20 Sep 1997	3	55	-5.09	0.41
25 Sep 1997	5	73	-4.86	0.46
4 Oct 1997	4	70	-1.95	0.54
3 Oct 1999	4	53	-4.74	0.35
7 Oct 2001	3	53	-1.26	0.7
3 Oct 2003	5	64	-4.45	0.51

Among 48 LT events in spring (Table 3), 47 of them were in April and only 1 was in May. Because spring is the season when stationary fronts occur frequently, bringing precipitation to the valley (Zhang and Wang 2008; Zhao et al. 2009; Zhu et al. 2011), among the 48 LT events, 46 were cold wet events ($R > 0.3$). The longest cold wet event ($R = 0.63$) in Table 3 started on 4 April 1993 and lasted for 11 days. There were 15, 11, 12, and 7 spring LT events in the 1960s, 1970s, 1980s, and 1990s, respectively. These numbers suggest a decreasing trend of spring LT events in the valley over the recent decades. Three special LT events, the two largest coverage cases on 1 October 2004 and on 3 October 1984 and a longest cold wet event starting on 4 April 1993, listed in the three tables will be used to examine their spatial structures and early signals.

4. Anomaly-based synoptic analysis

a. Autumn events

In the 17 autumn cold dry events, the one starting on 1 October 2004 had the largest spatial coverage (86 stations were affected) from 3 to 4 October 2004 in the mid- to lower Yangtze River valley. We choose this

event as an example, and use the anomaly-based method introduced in section 2b to examine the weather conditions from 1 to 8 October 2004 and to detect early synoptic disturbances for this cold dry event. The number of stations at which the surface air temperature fell below 20°C for at least three consecutive days and their average daily mean surface air temperature anomaly (SATA) series from 1 to 8 October 2004 are shown in Fig. 3a. The daily mean SATA at a station is defined by the difference between the observed daily mean surface air temperature and the climatic daily mean surface air temperature from 1979 to 2008. In this cold dry event, the lowest regional (with 86 stations) daily mean SATA was -4.93°C, recorded on 3 October 2004. The distribution of the SATA on 3 October 2004 (peak intensity of this event) is shown in Fig. 3b. There were three surface LT centers (LTCs), in the upper Yellow River valley, the upper Yangtze River, and the mid- to lower Yangtze River valley, respectively. We focus on the processes affecting the valley inside our study region (Fig. 1).

Analyzing the conventional synoptic charts, we found that on 23 September 2004 there was a trough in geopotential height along with cold temperature at 500 hPa over Siberia (60°N, 90°E). By 0000 UTC 1 October 2004, the height trough leading a temperature trough had propagated eastward to north China at 500 hPa (Fig. 4a). At 850 hPa (Fig. 4b), the height trough reached the east coast of China. The associated temperature trough was located to the west of the height trough, forming a flow pattern favorable for strong cold-air advection in the lower troposphere. At 0000 UTC 3 October 2004 (Fig. 4c), the cold-air advection at 500 hPa started to weaken when a tropical cyclone moved northward in the East China Sea (Fig. 4d). The SATA series in Fig. 3a is sensitive to the strengthening and weakening of cold-air advection, with a peak on 3 October 2004.

To demonstrate the utility of our anomaly-based method in capturing this LT event and its development, we show, in Fig. 5, the vertical cross sections of daily mean geopotential height and temperature along 115°E on 3 October 2004. Figure 5a presents the vertical cross section of the actual geopotential height and the temperature (gray solid and dashed lines, respectively) routinely used in daily weather analysis. In Fig. 5a, we also show the climatological values derived from 1979 to 2008 of the geopotential height and temperature on 3 October along the same cross section (thick solid and dashed lines, respectively). Relative to the climatological temperature line, the actual temperature shows a cold anomaly in the mid- to lower troposphere over the valley, while the magnitude and the spatial structure of this cold anomaly are unclear. The climatological height and the actual height have rather large basic values nearly equal

TABLE 3. As in Tables 1 and 2, but for the 48 regional LT events in late spring. The 20 events in boldface are used in individual and composite analyses. The event of the longest duration is highlighted in italics and is used as an example in the analysis.

Start date	Duration	Coverage	Intensity	Start date	Duration	Coverage	Intensity
11 Apr 1960	6	44	-2.66	20 Apr 1978	3	27	-3.07
6 May 1960	3	12	-2.45	1 Apr 1979	5	35	-2.4
2 Apr 1962	4	74	-4.57	13 Apr 1980	3	27	-4.9
10 Apr 1962	3	15	-1.43	24 Apr 1980	3	52	-2.79
6 Apr 1963	4	77	-5.49	2 Apr 1981	4	44	-2.5
18 Apr 1963	5	33	-1.42	3 Apr 1982	4	64	-3.09
6 Apr 1964	5	70	-4.21	8 Apr 1982	3	16	-2.44
3 Apr 1965	5	61	-2.97	15 Apr 1983	3	24	-2.34
10 Apr 1965	3	14	-2.09	5 Apr 1984	8	28	-2.44
4 Apr 1966	9	39	-2.53	4 Apr 1985	3	12	-1.88
4 Apr 1967	3	11	-1.68	1 Apr 1987	3	14	-4.15
10 Apr 1967	9	37	-1.64	11 Apr 1987	6	86	-3.51
9 Apr 1968	3	19	-4.26	6 Apr 1988	3	33	-4.33
3 Apr 1969	4	76	-5.48	11 Apr 1989	4	30	-1.54
16 Apr 1969	3	16	-3.62	3 Apr 1990	3	15	-3.15
10 Apr 1970	5	42	-1.95	4 Apr 1993	11	66	-3.66
16 Apr 1971	3	15	-1.78	9 Apr 1994	3	39	-2.82
1 Apr 1972	4	30	-5.93	1 Apr 1995	4	25	-2.48
7 Apr 1972	4	46	-2.84	1 Apr 1996	5	30	-3.89
1 Apr 1973	4	19	-2.9	8 Apr 1996	8	64	-2.25
1 Apr 1974	3	15	-3.35	3 Apr 1997	3	15	-3.4
1 Apr 1975	3	10	-2.37	25 Apr 2002	4	30	-1.68
2 Apr 1976	4	41	-3.52	9 Apr 2005	3	16	-1.39
7 Apr 1976	5	35	-1.74	12 Apr 2006	4	48	-3.72

to each other, so their differences are too small to indicate the cold event clearly. A slight difference between the climatological height (heavy solid line) and the actual height (gray solid line) marked by an arrow in Fig. 5a can be found near 200 hPa over the valley.

In contrast, such deviations are clearly shown in Fig. 5b by the anomalies in geopotential height and temperature on 3 October 2004 from their climatological means for that day. These anomalies unequivocally show a strong cold-air pool over the valley on 3 October 2004. The capability shown in Fig. 5b demonstrates the utility of this approach for revealing an LT event. As shown, this particular event was part of such an anomalous synoptic system, which had a negative center of geopotential height anomalies in the upper troposphere, a negative (cold) center of temperature anomalies in the middle troposphere, and another cold center in the lower troposphere. It is noted that the anomalous surface cold air and high pressure were coupled with a negative center of height anomalies in the upper troposphere. The strong negative height anomalies in the upper troposphere were related to the strong cold-air mass (negative temperature anomaly) below it, as required by the hydrostatic balance. The vertical structure of a negative center of height anomalies at the upper troposphere, a positive center of height anomalies near the cold temperature surface, and a cold-air column between these two centers is a typical vertical pattern, namely the LT vertical pattern,

for the LT events in the valley. To the north of the LT vertical pattern, there was a positive center of height anomalies, which will be useful in distinguishing between cold dry and cold wet events. This anomalous structure of height and temperature in Fig. 5b is also observable in the conventional synoptic chart in Fig. 5a but it can hardly be directly distinguished. The similar structures of the height and temperature anomalies can also be observed from the anomaly-standardized synoptic chart, but the intensities and the locations of the centers of the height and temperature anomalies show little difference when compared with those shown in Fig. 5b.

These striking differences from the analysis of the vertical profile of the anomalies in geopotential height and temperature suggest that it is possible to trace, by this method, the early development and propagation of the set of negative temperature anomalies in the mid- to lower troposphere and a negative center of height anomalies in the upper troposphere (Qian and Zhang 2012; Zhang and Qian 2012). From daily height and temperature anomalies, their maximal centers of standard deviation are respectively located between 200 and 300 hPa and around 850 hPa in the middle and high latitudes. Using this method, such anomaly centers in the troposphere are the target signals, or sources, for autumn LT events in the valley. For this event on 3 October 2004, a negative center of height anomalies at 300 hPa and a negative center of temperature anomalies at 850 hPa could be

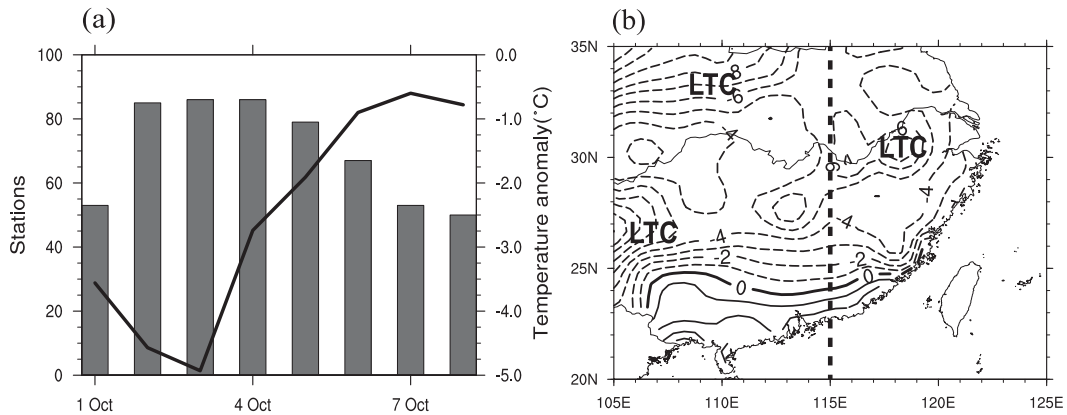


FIG. 3. A regional cold dry event from 1 to 8 Oct 2004 in the mid- and lower-Yangtze River valley. (a) Number of stations (bars) with daily mean temperature below 20°C, and their averaged daily mean SATA (solid line; °C). (b) Distribution of SATA (solid and dashed lines; 1°C interval) on 3 Oct 2004. LTC indicates the low-temperature centers. The heavy dashed line marks the 115°E longitude along which vertical cross sections will be analyzed.

traced back day by day until 23 September 2004, where it is located in Siberia (60°N, 90°E). As depicted in Fig. 6a, a pair of negative centers of temperature anomalies at 850 hPa and height anomalies at 300 hPa were established on 23 September 2004. They propagated southeastward into eastern China on 1 October 2004 (Fig. 6d), causing the particular LT event in the

valley. In Figs. 6d and 6e, the center of the height anomalies at 300 hPa was located in northern China, while a cold center at 850 hPa extended to the mid- and lower Yangtze River. The location of the negative temperature anomaly center in the lower troposphere located to the south of the height anomaly center in the upper troposphere can be clearly observed in Fig. 5b. This

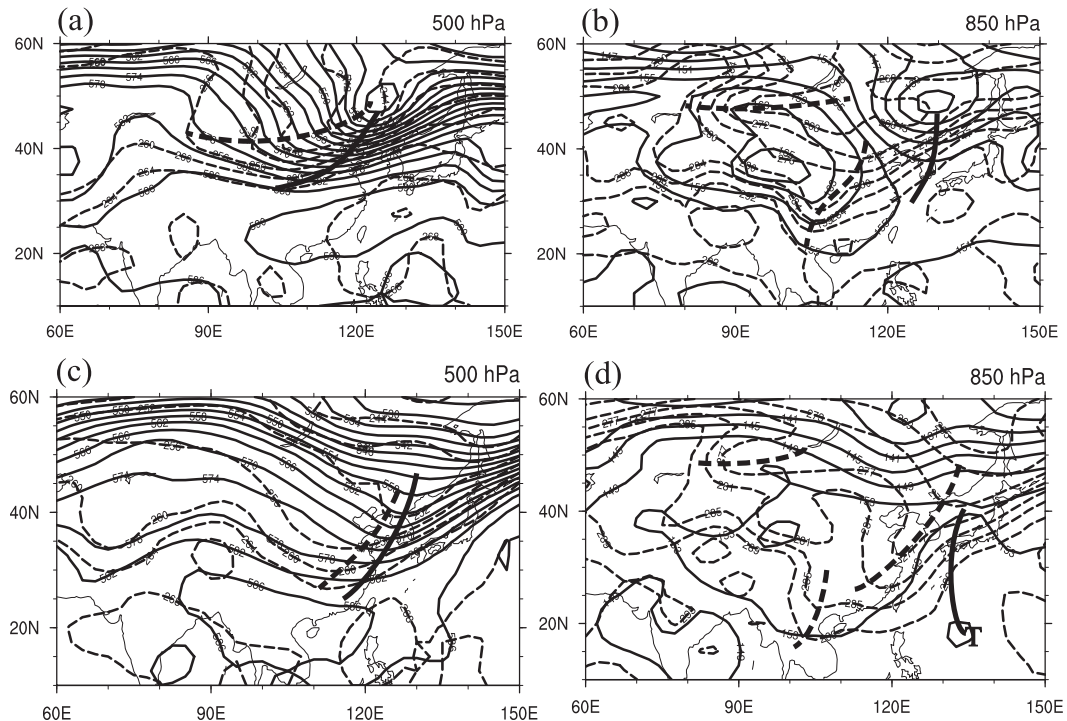


FIG. 4. Conventional synoptic charts. Geopotential height (solid line; 40-gpm interval) and temperature (dashed line; 4-K interval) at (a) 500 and (b) 850 hPa at 0000 UTC 1 Oct 2004. (c),(d) As in (a) and (b), but for 3 Oct 2004. The heavy solid (dashed) line indicates the geopotential height (temperature) trough. The letter T in (d) indicates the location of a tropical cyclone.

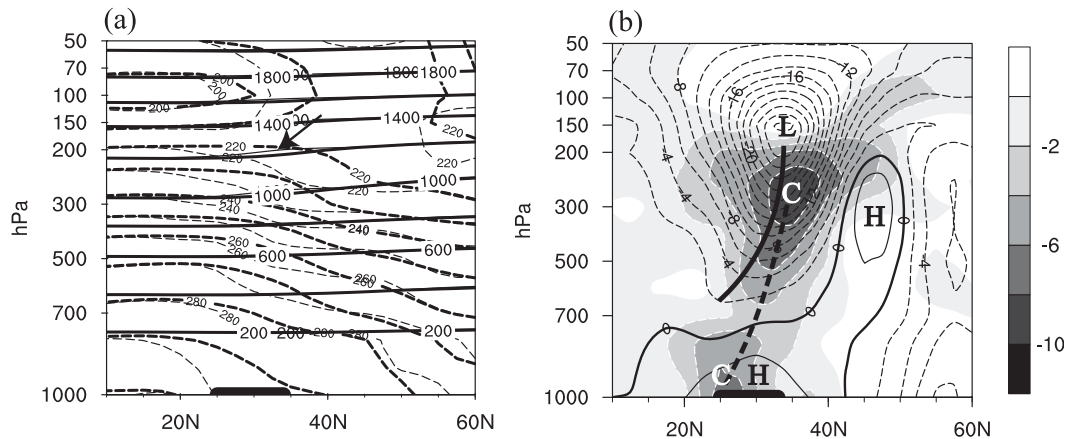


FIG. 5. Vertical cross section of geopotential height and temperature on 3 Oct 2004. (a) Actual and climatic height (gray and heavy solid lines; 2000-gpm interval), and actual and climatic temperature (gray and heavy dashed lines; 10-K interval). (b) Anomalies of geopotential height (solid and dashed lines; 20-gpm interval) and temperature (grayscale; 2-K interval) along 115°E on 3 Oct 2004. The mid- to lower-Yangtze River valley is highlighted by the heavy solid line along the abscissa. In (a), the arrow indicates the difference between the actual and climatic heights, i.e., between the gray and heavy solid lines. In (b), the thick solid (dashed) line indicates the trough in height (temperature) anomalies. Letters H and L mark the positive and negative centers in height anomalies, respectively, and C is the center of the negative temperature anomalies. In (b), white areas are positive temperature anomalies.

example shows that the negative centers of temperature anomalies at 850 hPa and height anomalies at 300 hPa from the region in eastern China can be traced back about 8 days to Siberia. However, another pair of negative centers of temperature anomalies at 850 hPa and height anomalies at 300 hPa in western Europe gradually weakened from 23 September (Fig. 6a) to 25 September (Fig. 6b) and finally dissipated on 29 September (Fig. 6c). These signals, if present in a forecast model, may provide forecasters early warning information for a potential LT event.

Additional analyses of the vertical structure and horizontal distribution of height and temperature anomalies, as done from the above case, were completed for 16 additional autumn cold dry events in the valley. Among the total of 17 dry events, 20 early signals of initial disturbances were traced with pairs of negative centers of height and temperature anomalies at 300 and 850 hPa, respectively. Their initial locations are shown by the open dots in Fig. 7a. Seventeen of these cases developed further, amplifying while propagating into eastern China where they resulted in 17 cold dry events. Among them, three initial disturbances merged with others during their propagation processes. Many remote disturbances in our searching domain did not propagate to eastern China. The evolution of the initial disturbance marked by a black triangle in Fig. 7a is the case illustrated in Fig. 6 and in October 2004 caused the largest coverage among dry events. The average length of time from the disturbance initiation to the occurrence of cold dry events in the valley is 12.5 days, a remarkable lead time for indicating those events.

A composite of vertical cross sections along 115°E is shown in Fig. 7b for all 17 of the cold dry events when their initial disturbances amplified and arrived at the solid dot locations in Fig. 7a. The vertical structure in Fig. 7b has all the key features described in Fig. 5b, indicating a strong cold temperature anomaly centered near 850 hPa, underneath a negative anomaly center of the geopotential height between 200 and 300 hPa. A center of cold high pressure is shown near the surface in the valley. The LT vertical pattern is also clearly observed from this dry composite of 17 cases with a positive center of height anomalies to its north in the upper troposphere.

As a special case suggested in section 3b, the wet event with the largest coverage occurred from 3 to 10 October 1984 and influenced a broad area (86 stations) in the mid- to lower Yangtze River valley. This event is also examined using the anomaly-based synoptic analysis method. In this wet LT event, the lowest regional daily mean SATA was -5.43°C , with $R = 0.73$, which peaked on 5 October 1984 (Table 2 and Fig. 8a). The regional distribution of the SATA on 5 October 1984 is shown in Fig. 8b. A major LT center (indicated by LTC) is located to the south of the Yangtze River.

For this cold wet event, its cold-air advection at 500 hPa (Fig. 9a) is weaker than that in the cold dry event shown in Fig. 4a. This weak cold-air advection from the northwest, and the warm air mass to the south, allowed for the formation of a lower-tropospheric stationary front. Several isothermal lines are zonally oriented along the Yangtze River from 3 to 5 October 1984 (Figs. 9b and 9d). The stationary front brought cold rain

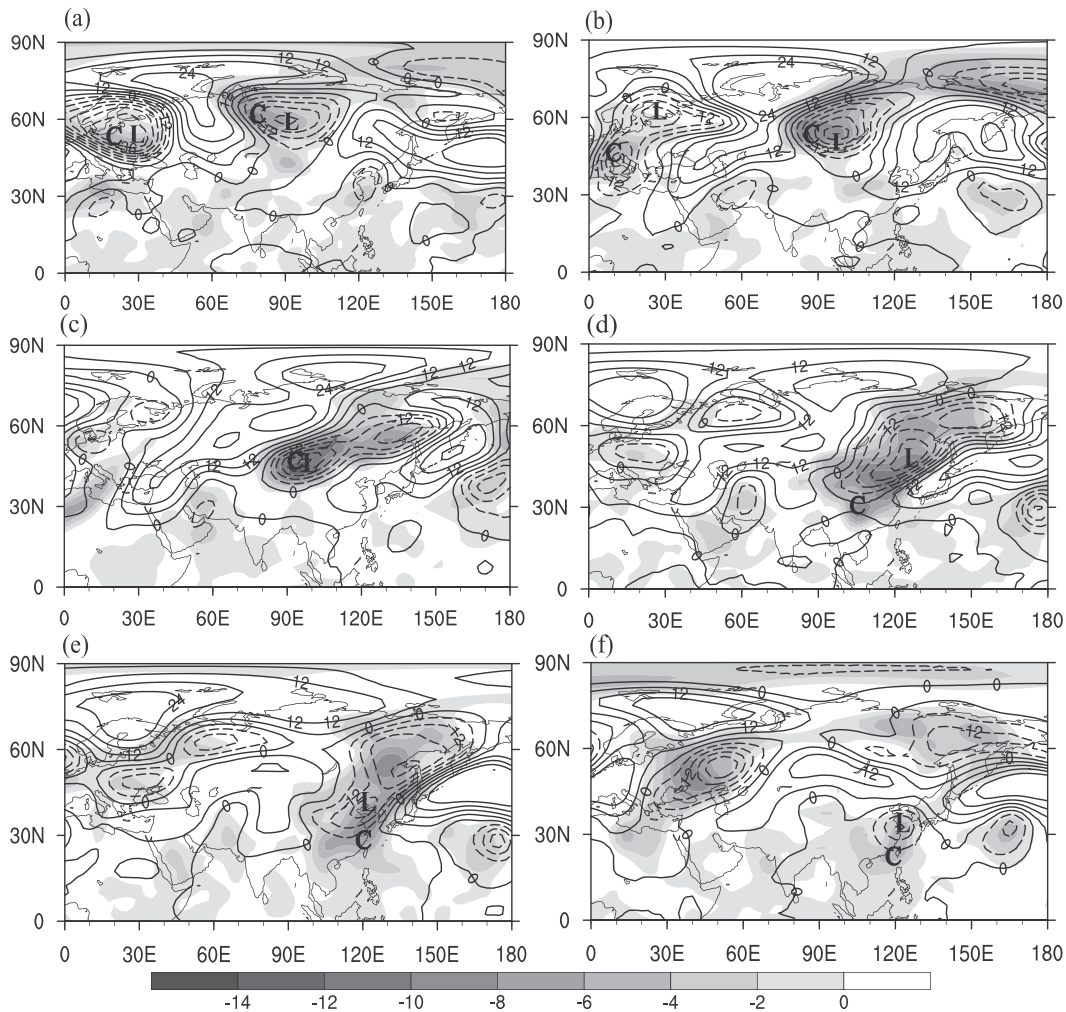


FIG. 6. Anomaly-based synoptic charts showing the anomalies (positive, solid line; negative, dashed line; 60-gpm interval) of geopotential height at 300 hPa, and the anomalies (shading; 2-K interval) of temperature at 850 hPa on (a) 23 Sep, (b) 25 Sep, (c) 29 Sep, (d) 1 Oct (starting date for this LT event in the valley), (e) 2 Oct, and (f) 4 Oct 2004. Letters L and C indicate the negative centers of the height anomalies at 300 hPa and the negative centers of the temperature anomalies at 850 hPa, respectively. White areas represent the positive temperature anomalies.

and anomalously low temperatures to the mid- to lower Yangtze River valley. Similarly, we show two vertical cross sections along 115°E for this cold wet event in Fig. 10, with Fig. 10a showing the cross section constructed from the traditional analysis approach and Fig. 10b showing the cross section constructed from the anomaly-based method. Again, Fig. 10b reveals the axis of cold temperature anomalies extending from a negative center of height anomalies at 300 hPa to a positive center of height anomalies near the surface. The LT vertical pattern is also noted over the valley, but there was a negative center of height anomalies in the upper troposphere over northern China and a weak warm temperature anomaly in its south. This feature of a wet event is different from that of the dry event shown in Fig. 5b.

The centers of the height anomalies at 300 hPa and temperature anomalies at 850 hPa in Fig. 10b could also be traced back day by day to a disturbance featured with a pool of anomalously cold air in northern Europe (70°N , 55°E) on 24 September 1984 (Fig. 11). On 24 September 1984, there were five large centers of disturbances over the Eurasian continent (Fig. 11a). Among them, a pair of negative centers that arrived in northeast China and whose cold air influenced northern China. However, only the one from northern Europe amplified and propagated southeastward to northern China on 2 October 1984 (Fig. 11d). From 2 to 4 October, this air mass of strong cold temperature anomalies split into two centers, and one of them moved south into eastern China and caused the cold wet event in the valley. The results in

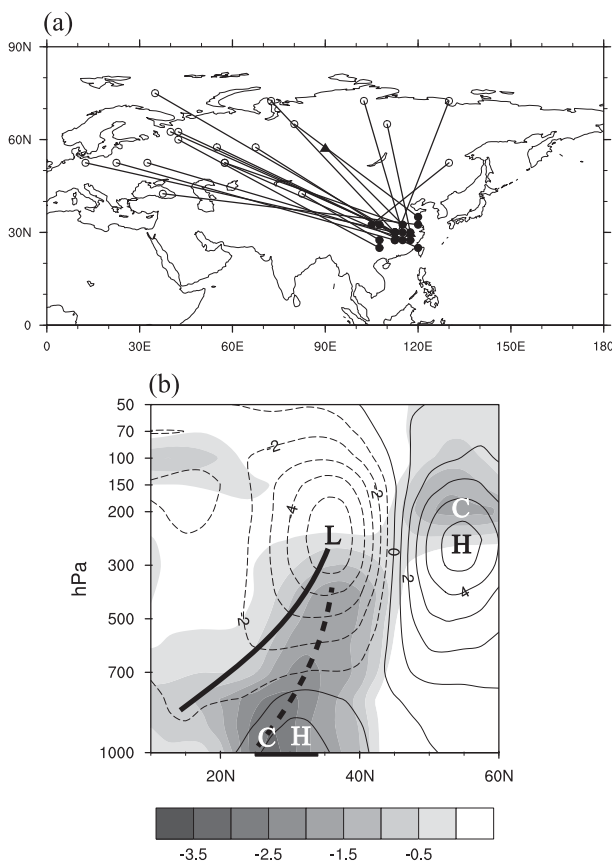


FIG. 7. (a) Locations of initial disturbances in geopotential height and temperature (20 open dots) and the corresponding positions of 17 autumn cold dry events (solid dots), based on the signal tracing from anomalies of height and temperature. The black triangle indicates the case shown in Figs. 5 and 6. (b) Composite vertical cross section of height anomalies (solid and dashed lines; 10-gpm interval) and temperature anomalies (shading; 0.5-K interval) along 115°E longitude of the 17 cold dry events. The thick solid (dashed) line indicates the trough of height (negative temperature) anomalies. White areas are positive temperature anomalies.

Fig. 11 also confirm that the pair of negative centers of temperature anomalies at 850 hPa and height anomalies at 300 hPa serve as an early indication of disturbances that can develop while propagating into China and cause a cold wet event in the valley with a lead time of about 9 days.

For all the cold wet LT events listed in Table 2, 30 pairs of initial disturbances of negative height anomalies at 300 hPa and negative temperature anomalies at 850 hPa were identified and traced, as is shown in Fig. 11. Their geographical locations are shown by the open circles in Fig. 12a. Of those initial disturbances, 27 amplified while propagating into the eastern China and caused cold wet events in the valley (marked by solid dots in Fig. 12a). Three initial disturbances merged with the other ones during their propagations. The average

time length between the appearance of the initial disturbances and the occurrence of the cold wet events in the valley is 8.8 days. The composite of the vertical cross sections for these autumn cold wet events is shown in Fig. 12b, delineating features similar to those in Fig. 7 for autumn cold dry events. The LT vertical pattern with a negative center of height anomalies at the upper troposphere, a positive center of height anomalies near the cold surface, and a cold-air column between these two centers is also typical of the patterns found in the mid- to lower Yangtze River valley. There are major differences between the cold dry and cold wet events in autumn. Comparisons of Figs. 7b and 12b reveal the following: (i) the cold dry events have a much larger body of cold air in the valley than the cold wet events; (ii) in the cold dry events, there is a positive center of height anomalies located along the north side of the cold-air column; and (iii) a weaker positive height anomaly region is found on the south side of the cold-air column in the cold wet events. In the former, the positive height anomaly on the north pressures the cold air mass deep into southern China (Fig. 7b). In the latter, the contrast of pressure in the valley forms a stationary front and favors precipitation (Fig. 12b).

Between the 17 cold dry and 27 cold wet events in autumn over the study period, the similarities and differences in their composite horizontal temperature and relative humidity trends in the lower troposphere (850 hPa) are compared in Fig. 13. In the composite distribution of temperature anomalies, a similarity between the cold dry and cold wet events (cf. Figs. 13a and 13b) is that they both have a temperature trough extending from northeast China to the Yangtze River valley. One of the differences is shown by the squash shape of the temperature anomaly in the cold dry cases (Fig. 13a) while an upside-down squash-shaped temperature anomaly for the cold wet cases is shown in Fig. 13b in China. This difference shows that the center of the negative temperature anomalies of the dry cases is slightly lower in latitude than that of the wet cases so that the southern edge of the dry anomaly has reached the south China coast. Thus, the former stronger cold air can extend deeper into southern China causing colder dry LT events and the further southward spread of the cold air also prevents stationary front formation in that region. The latter condition is favorable for forming a stationary frontal zone between the cold-air mass to the north and the warmer moisture air mass to the south for the cold wet event. This difference in temperature anomalies is further confirmed by the contrasting relative humidity anomalies at 850 hPa between the composited cold dry and cold wet events shown by two opposite centers of “D” and “W” in Figs. 13e and 13f.

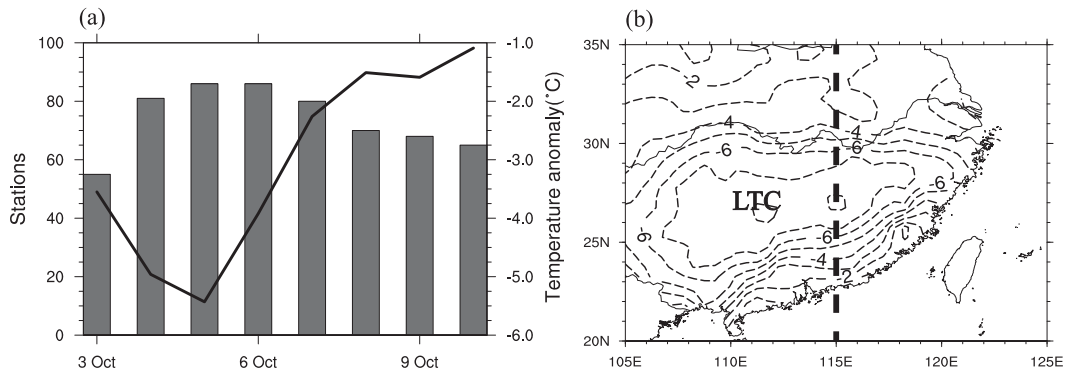


FIG. 8. As in Fig. 3, but for the cold wet event occurring from 3 to 10 Oct 1984 south of the Yangtze River.

b. Late spring LT events

As described in section 3b, there were 46 cold wet events ($R > 0.3$) among the total of 48 LT events in spring during the study period of 1960–2008 (Table 3). Most weather systems in spring in southern China are characterized by interactions between air masses of contrasting temperatures and moisture, and their associated precipitation. Thus, for the spring LT events, we only focus on the cold wet events. Among the 46 late spring cold wet events, the longest duration is the case from 4 to 14 April 1993, which covers about 11 days. It happened when a stationary front became established in the Yangtze River valley ($R = 0.63$). In Fig. 14, a set of

figures similar to Fig. 3 is presented to illustrate the process and influence of this particular cold wet event. Figure 14a shows the number of stations affected by this wet event and the time series of their averaged daily surface air temperature anomaly. On 4 April (the starting date), there were 56 stations affected by the low temperature. The lowest temperature was reported on 5 April at 62 stations in the valley, with the daily SATA -3.66°C . The spatial distribution of the SATA on 5 April 1993 is shown in Fig. 14b. There were two LTCs: one in the mid-to lower Yangtze River valley and the other in the upper Yellow River valley. The temperature anomaly at the LTC in the Yangtze River valley reached -6°C on 5 April 1993. Although the affected region diminished

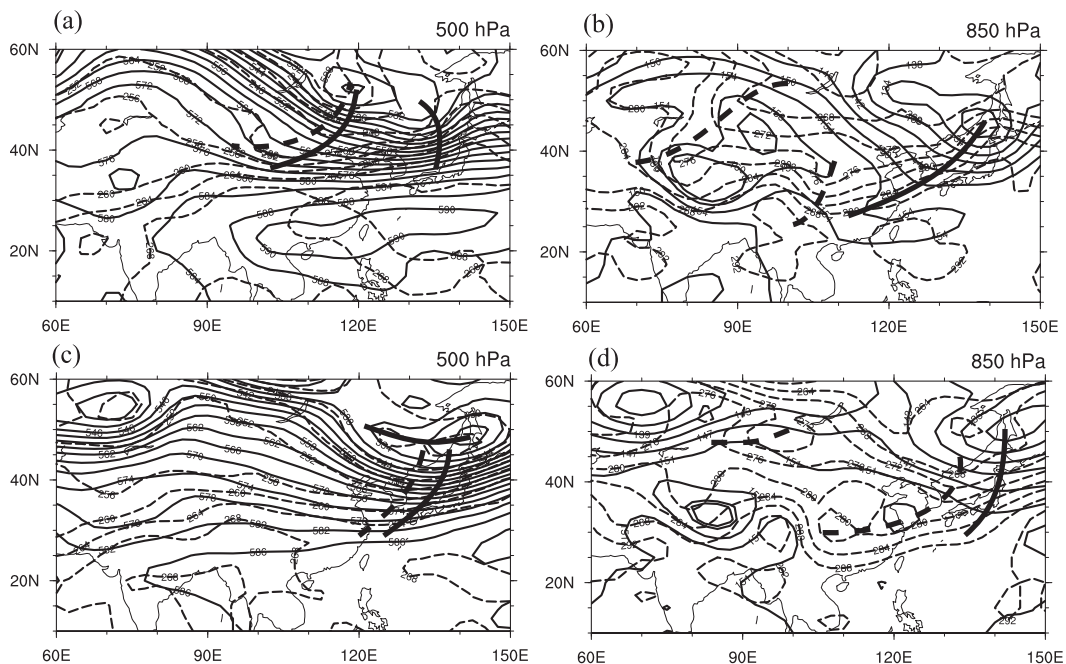


FIG. 9. As in Fig. 4, but for (a) 500 and (b) 850 hPa at 0000 UTC 3 Oct 1984, as well as for (c) 500 and (d) 850 hPa at 0000 UTC 5 Oct 1984.

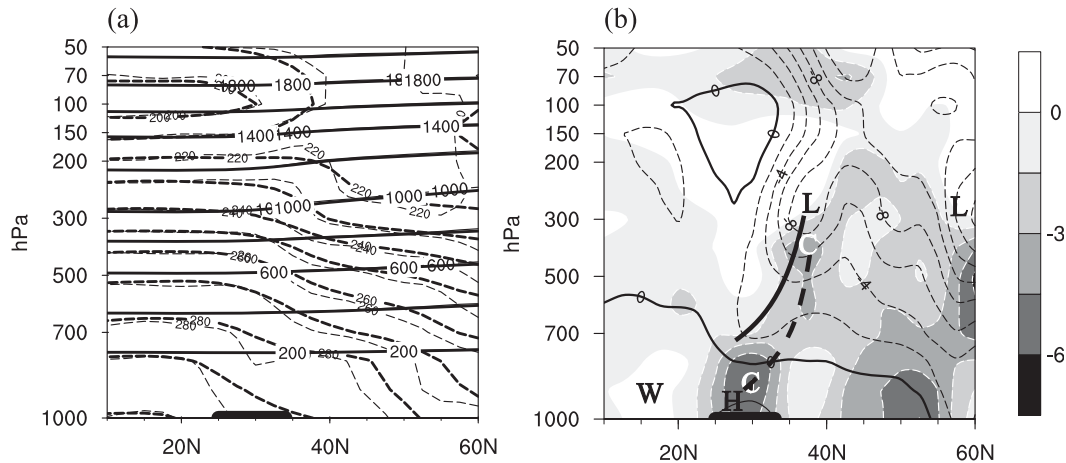


FIG. 10. As in Fig. 5, but for the cold wet event on 5 Oct 1984. In (b), the letter W denotes a weak warm center.

after 6 April, the other two cooling processes peaked on 8 and 12 April 1993, extending the LT event's duration. Clearly, the persistence of the LT events in this case was caused by three cooling processes. A similar case is the LT freezing-rain event that occurred in southern China from 10 January to 2 February 2008, undergoing four cooling processes (Qian and Fu 2010).

In Fig. 15, we show a similar comparison between the cross sections of the temperature and geopotential height derived from the conventional analysis method (Fig. 15a) and that derived from our anomaly-based method (Fig. 15b). The difference between these cross sections is outstanding. Again, results from the anomaly-based method clearly depict the cold wet event whereas the results from the conventional method give a rather fuzzy description of the event. In Fig. 15b, the LT vertical pattern with a set of a negative height anomaly centered at around 300 hPa and a negative temperature anomaly centered at 850 hPa indicates unequivocally the cold wet event. Interestingly, vertical profile of anomalies for this cold wet event (Fig. 15b) is nearly identical to the composite profile for cold wet events in autumn (Fig. 12b). The similarity that a weaker positive height anomaly is on the south side of the cold-air column suggests the consistency of these cold wet events in the mid- to lower Yangtze River valley in spring and autumn.

Again, using the anomaly-based method, we can trace the early disturbances for this spring cold wet event in the valley. The results show a pair of negative centers of height anomalies at 300 hPa and temperature anomalies at 850 hPa in northwest Asia (50°N, 80°E) on 29 March (Fig. 16a). As shown by the sequence in Fig. 16, the negative center of height anomalies marked by the L and the negative center of temperature anomalies marked by the C on 29 March amplified while propagating southeastward. When arriving in eastern China

(Fig. 16d), this maturing disturbance caused the cold wet event and resulted in the first peak on 5 April (Fig. 14a) in the Yangtze River valley. It is interesting to note that in this particular event, there was another mass of strong cold air descending from northern Siberia to eastern China (Figs. 16d–f). This air mass arrived at the valley on 8 April and reinforced the coldness, resulting in its second peak on 8 April (Fig. 14a). In our previous study for the persistence of LT freezing-rain events in 2008 (Qian and Zhang 2012), four negative centers at 850 hPa consecutively marched along a similar path and arrived in southern China under a stable large-scale circulation regime in the upper troposphere (a negative height anomaly at 300 hPa). The persistence of this cold wet event in spring was also caused by three negative centers of temperature anomalies that arrived in eastern China one after another under a large negative center of height anomalies at 300 hPa in northern China. In Figs. 16e,f, C1, C2, and C3 indicate three cold turbulences at 850 hPa, which consecutively reached the valley.

Among the 46 cold wet events in late spring (Table 3), there were 20 cases with averaged daily SATAs colder than -3.0°C . We examine these events using the anomaly-based method to trace the initial disturbances that developed and caused those events. Figure 17a shows the geographical locations of initial disturbances in the height anomalies at 300 hPa and the temperature anomalies at 850 hPa that caused those 20 spring LT events. The average lead time length from the appearance of initial disturbances to the occurrence of the 20 spring LT events in the valley is 6.9 days. The earliest disturbance is identified 13 days ahead of the spring LT event. The initial location of the disturbance resulting in the case from 4 to 6 April 1993 is marked in Fig. 17a by the black triangle.

The LT vertical pattern composited over the 20 strong spring wet events is comparable to the composite

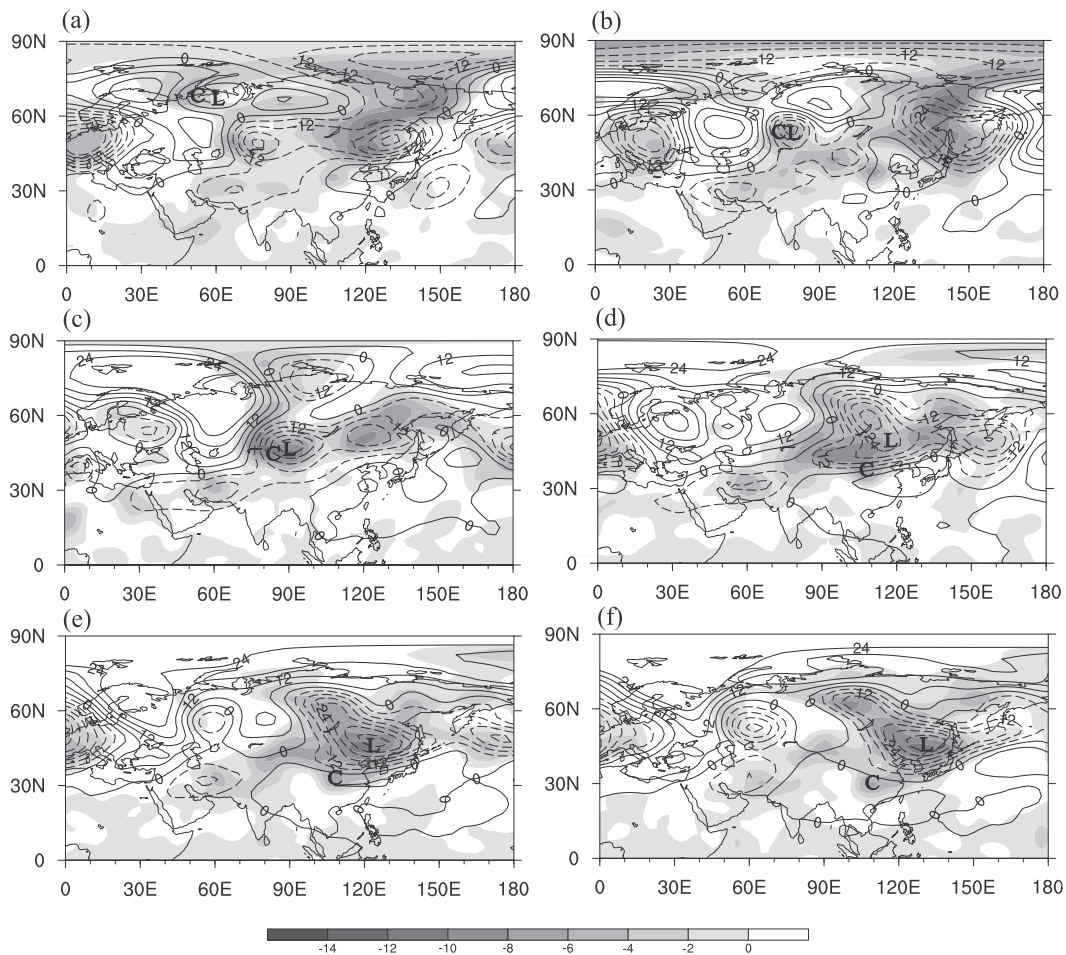


FIG. 11. As in Fig. 6, but on (a) 24 Sep, (b) 27 Sep, (c) 30 Sep, (d) 2 Oct, (e) 3 Oct (starting date of the event), and (f) 4 Oct 1984.

pattern for the cold wet events in autumn (cf. Figs. 17b and 12b). Detailed comparisons further indicate that the spring cold wet events are less vigorous than the cold wet events in autumn (see the difference in temperature scales between Figs. 17b and 12b). Their differences near the surface height anomalies further suggest that the cold air in the spring events is shallower and more concentrated in the lower portion of the troposphere.

5. Summary

The agriculture in the mid- to lower Yangtze River valley in China has a double rice cropping system, that is, rice is grown and harvested in spring and autumn each year. Because spring and autumn are the transition seasons, from cold to warm in the former and the reverse in the latter, low-temperature events have historically been a major threat and hazard to rice production. In spring, the LT events are mostly cold wet events, with low temperatures and precipitation. In autumn, cold wet

events account for nearly one-half of the LT events. The other half are cold dry events, which are colder with strong northerly winds but without precipitation. These LT events can only be vaguely indicated by current conventional weather analysis methods, and cannot be predicted with reasonable lead times useful to farmers. It has been a challenge to develop effective methods to better describe those events and improve the lead times of their predictions.

In this study, we showed a new anomaly-based method that can single out the key features of both the wet and dry LT events. Moreover, by tracing those features to their initial development, this method is demonstrated to advance predictions of the LT events by a lead time much longer than the current conventional methods.

Using the anomaly-based method to examine synoptic charts, we can construct horizontal maps and vertical cross sections of temperature and geopotential height anomalies. From those anomalies we can reveal the spatial scale and intensity of both the wet and dry LT events. We found

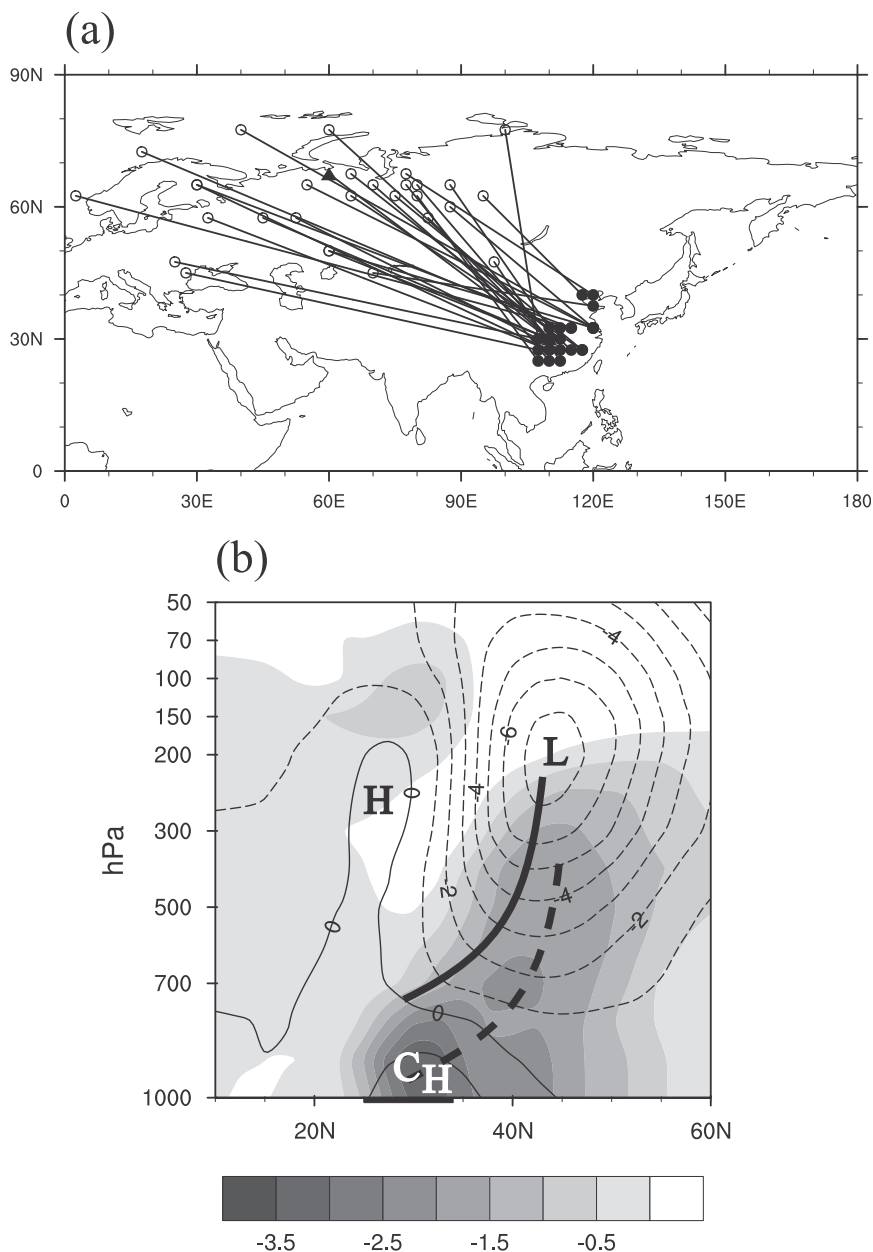


FIG. 12. As in Fig. 7, but for 27 cold wet events in autumn. The black triangle in (a) indicates the case shown in Figs. 10 and 11.

that the vertical anomaly profile showed a negative center of height anomalies in the upper troposphere, a positive center of height anomalies near the cold surface, and a cold-air column between these two centers, which is a signature of the vertical anomaly pattern for LT events (or for their further development).

With presence of this vertical pattern, the surrounding horizontal anomaly pattern determines if a LT event will be wet or dry. If a positive center of height anomaly is to the north of this cold-air column, a cold dry event will

most likely develop. If a positive height anomaly is to the south of the cold-air column, a cold wet event with precipitation will most likely occur in the valley. Detailed analyses of these features on daily anomaly charts must be carefully examined to search for, identify, and follow negative centers of temperature anomalies under a negative center of height anomalies in the upper troposphere, as well as the horizontal anomaly patterns in making predictions of the LT events in the Yangtze River valley.

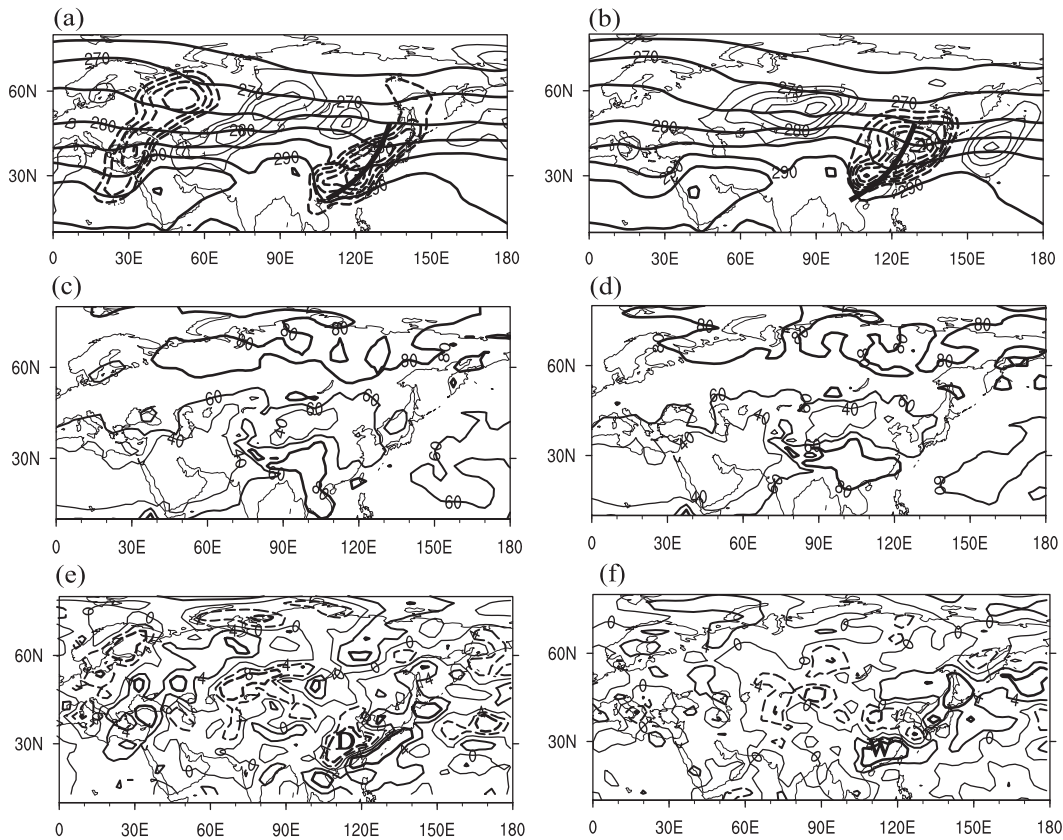


FIG. 13. Composites of temperature and relative humidity at 850 hPa. Climatic temperature (thick-solid line; 5-K interval) and averaged temperature anomalies (thin solid and dashed lines; 0.5-K interval) of (a) 17 cold dry events and (b) 27 cold wet events. (c),(d) As in (a) and (b), but for relative humidity (%). (e),(f) As in (a) and (b), but for humidity anomalies (%). In (a) and (b), the heavy solid line marks the temperature trough. In (e) and (f), the letters D and W denote the centers of negative (dry) and positive (wet) humidity anomalies, respectively, in the Yangtze River valley.

This anomaly-based method and a tracing procedure have been applied to real cases: 20 strong spring LT events and 44 autumn LT events occurring in 1960–2008. Results showed that the method can trace the initial synoptic disturbances of those events

and can follow their development as they evolve into the LT events in the Yangtze River valley. For the 44 autumn events, the average lead time, from the date when the initial disturbances were identified to the date when LT events occurred in the valley, is

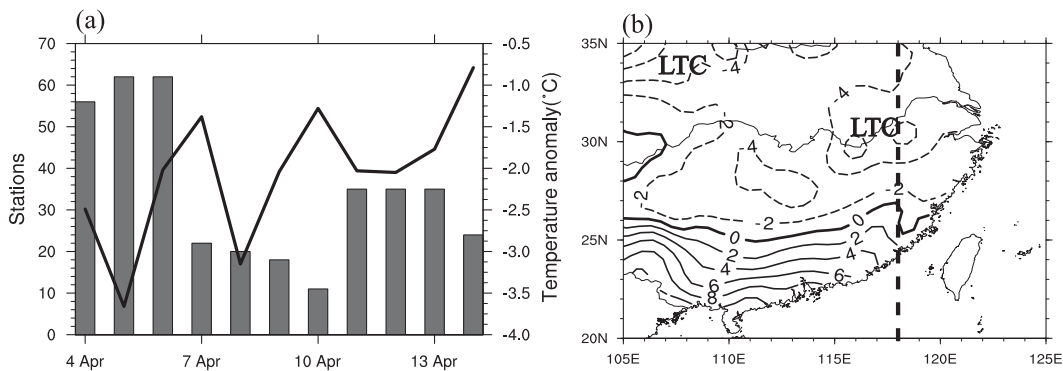


FIG. 14. As in Fig. 3, but for (a) the spring cold wet event from 4 to 14 Apr 1993 and (b) the distribution of SATa (°C) on 5 Apr 1993.

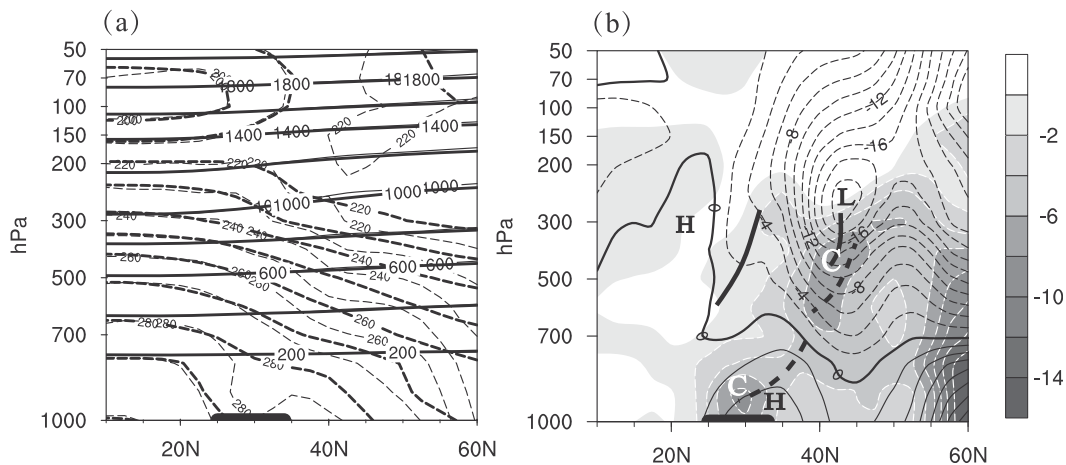


FIG. 15. As in Fig. 5, but for the spring cold wet event on 5 Apr 1993 and along 117.5°E.

10.2 days. For the 20 strong spring LT events, the average leading time from the appearance of initial disturbances to the occurrence of LT events in the valley is 6.9 days.

These results warrant a proposal for an effective method of improving the LT event prediction in the mid- to lower Yangtze River valley in China. Using this method, one should be able to identify the early

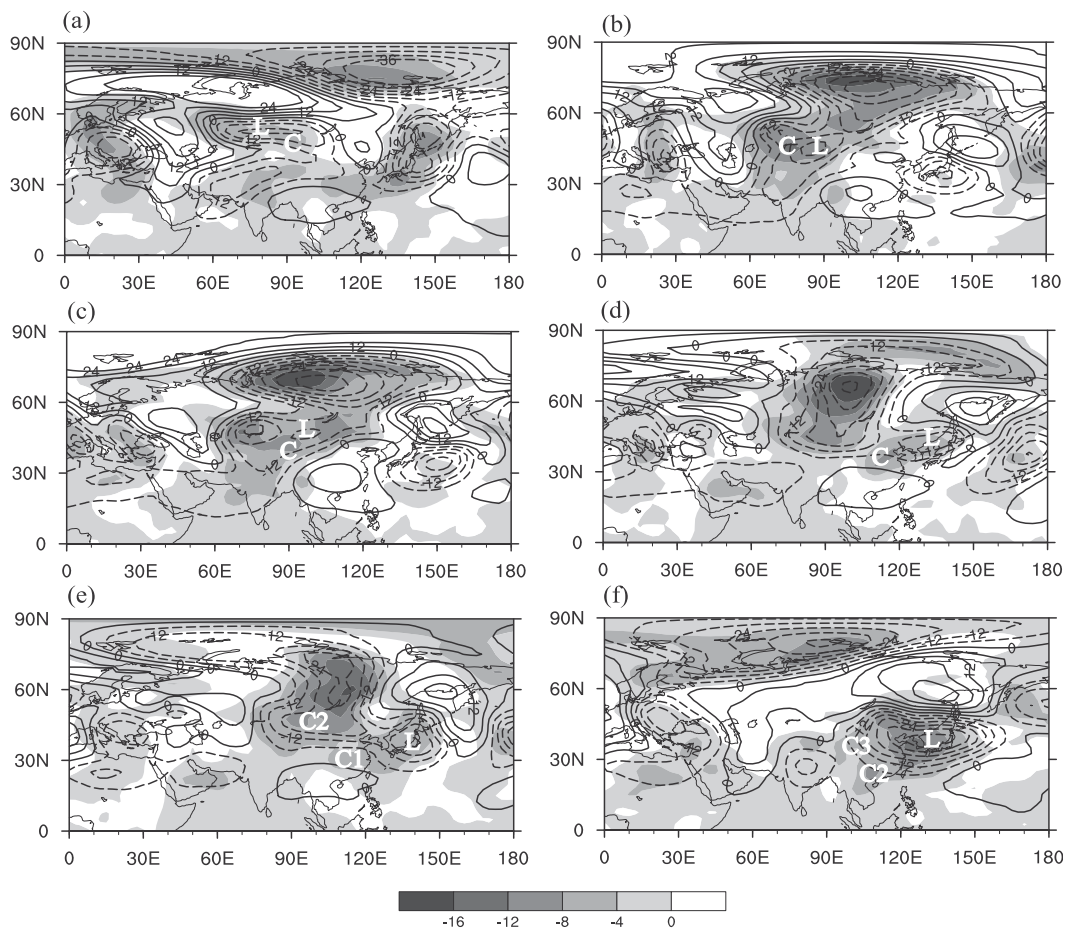


FIG. 16. As in Fig. 6, but for the event from 4 to 14 Apr 1993 on (a) 29 Mar, (b) 1 Apr, (c) 2 Apr, (d) 4 Apr (starting date), (e) 5 Apr, and (f) 8 Apr. In (e) and (f), letters C1, C2, and C3 indicate three centers of the temperature anomalies at 850 hPa.

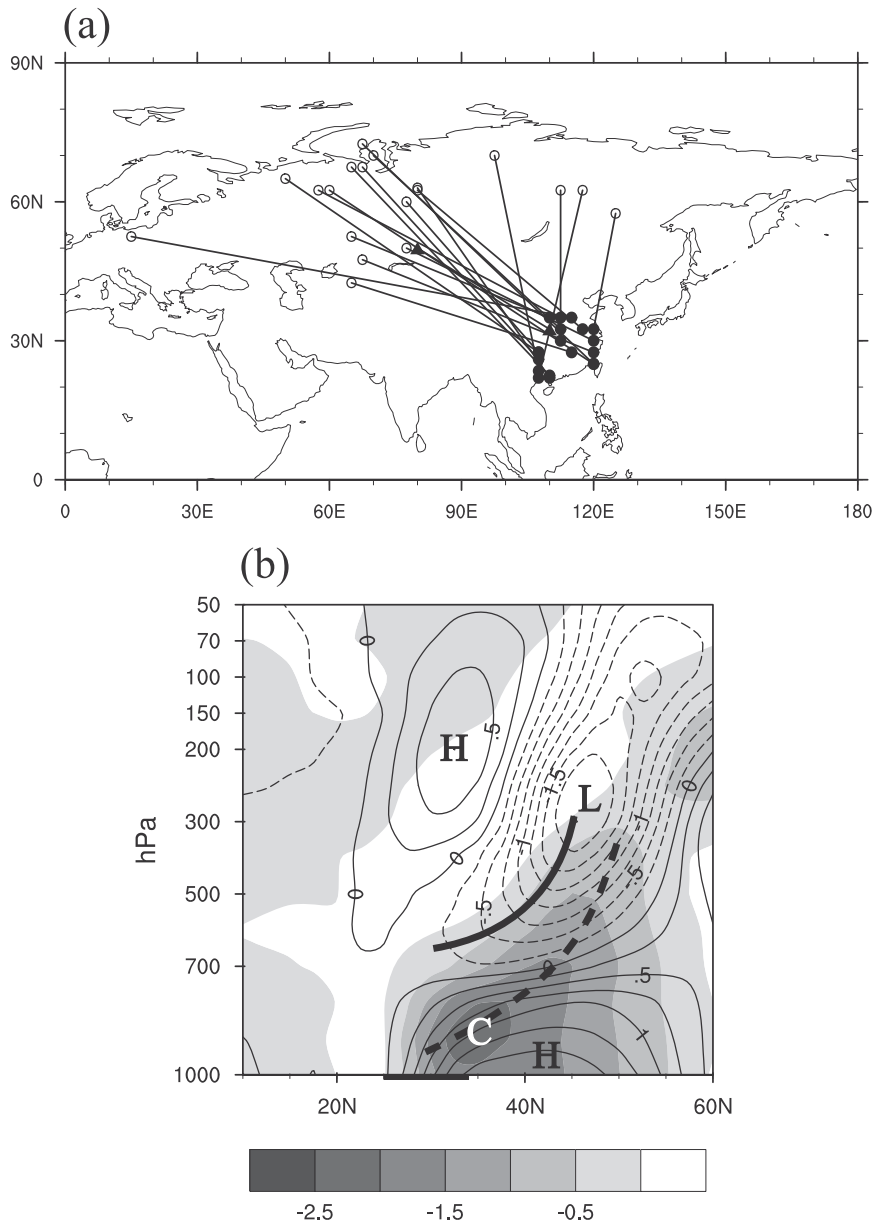


FIG. 17. As in Fig. 7, but for 20 strong cold wet events in spring. In (b), the contour interval of the geopotential height anomalies is 2.5 gpm.

disturbances in geopotential height in the upper troposphere and temperature anomaly in the lower troposphere from the predictions produced by operational NWP models, such as ECMWF and NOAA GFS. Using these disturbances as the primary precursors, it is possible to improve the performance of the medium- to extend-range forecasts of LT events in the Yangtze River valley. In autumn, attention should also be given to the details of the vertical profile of the geopotential height anomalies, which will help distinguish the cold wet events from the cold dry events.

Acknowledgments. The authors thank the editor and three reviewers for their comments and suggestions, which helped improve the clarity of this paper. Figures 2, 4, 9, and 13 were prepared following the suggestions of the reviewers. This work is supported by the National Natural Science Foundation of China (41375073) and the Key Technologies R&D Program (201306032), as well as the Strategic Priority Research Program of the Chinese Academy of Sciences (XDA0509400). The NCEP–NCAR reanalysis dataset was obtained online (<http://www.esrl.noaa.gov/psd/data/gridded/data.ncep.reanalysis.html>).

Author QH was supported by USDA Cooperative Research Project NEB-38-088.

REFERENCES

- Chen, F., S. B. Yang, S. H. Shen, M. Zhang, and Y. X. Zhao, 2013: Spatial and temporal distribution of spring cold damage in double cropping rice areas of the middle and lower reaches of the Yangtze River (in Chinese). *Jiangsu J. Agric. Sci.*, **29**, 540–547.
- Ding, T., and W. H. Qian, 2011: Geographical patterns and temporal variations of regional dry and wet heatwave events in China during 1960–2008. *Adv. Atmos. Sci.*, **28**, 322–337, doi:[10.1007/s00376-010-9236-7](https://doi.org/10.1007/s00376-010-9236-7).
- Ding, Y. H., Z. Y. Wang, Y. F. Song, and J. Zhang, 2008: Causes of the unprecedented freezing disaster in January 2008 and its possible association with the global warming (in Chinese). *Acta Meteor. Sin.*, **66**, 808–825.
- Du, J., R. H. Grumm, and G. Deng, 2014: Ensemble anomaly forecasting approach to predicting extreme weather demonstrated by extremely heavy rain event in Beijing (in Chinese). *Chin. J. Atmos. Sci.*, **38**, 685–699.
- Du, Y. D., 2005: Frost and high temperature injury in China. *Natural Disasters and Extreme Events in Agriculture*, M. V. K. Sivakumar, Ed., Springer, 145–157.
- Easterling, D. R., J. L. Evans, P. Y. Groisman, T. R. Karl, K. E. Kunkel, and P. Ambenje, 2000: Observed variability and trends in extreme climate events: A brief review. *Bull. Amer. Meteor. Soc.*, **81**, 417–425, doi:[10.1175/1520-0477\(2000\)081<0417:OVATIE>2.3.CO;2](https://doi.org/10.1175/1520-0477(2000)081<0417:OVATIE>2.3.CO;2).
- Feng, P. Z., and Coauthors, 1985: *China Major Meteorological Disasters Analysis*. Meteorology Press, 271 pp.
- Grumm, R. H., and R. Hart, 2001: Standardized anomalies applied to significant cold season weather events: Preliminary findings. *Wea. Forecasting*, **16**, 736–754, doi:[10.1175/1520-0434\(2001\)016<0736:SAATSC>2.0.CO;2](https://doi.org/10.1175/1520-0434(2001)016<0736:SAATSC>2.0.CO;2).
- Hart, R. E., and R. H. Grumm, 2001: Using normalized climatological anomalies to rank synoptic-scale events objectively. *Mon. Wea. Rev.*, **129**, 2426–2442, doi:[10.1175/1520-0493\(2001\)129<2426:UNCATR>2.0.CO;2](https://doi.org/10.1175/1520-0493(2001)129<2426:UNCATR>2.0.CO;2).
- Kalnay, E., and Coauthors, 1996: The NCEP/NCAR 40-Year Reanalysis Project. *Bull. Amer. Meteor. Soc.*, **77**, 437–471, doi:[10.1175/1520-0477\(1996\)077<0437:TNYRP>2.0.CO;2](https://doi.org/10.1175/1520-0477(1996)077<0437:TNYRP>2.0.CO;2).
- Lalurette, F., 2003: Early detection of abnormal weather conditions using a probabilistic extreme forecast index. *Quart. J. Roy. Meteor. Soc.*, **129**, 3037–3057, doi:[10.1256/qj.02.152](https://doi.org/10.1256/qj.02.152).
- Li, Z., and Z. W. Yan, 2009: Homogenized daily mean/maximum/minimum temperature series for China from 1960 to 2008. *Atmos. Ocean. Sci. Lett.*, **2**, 237–243.
- Qian, W. H., and J. L. Fu, 2010: Frontal genesis of moisture atmosphere during the early 2008 persistent freezing-rain event in southern China. *China Earth Sci.*, **53**, 454–464, doi:[10.1007/s11430-009-0101-4](https://doi.org/10.1007/s11430-009-0101-4).
- , and Z. J. Zhang, 2012: Precursors to predict low-temperature freezing-rain events in southern China. *Chin. J. Geophys.*, **55**, 1501–1512.
- , J. Li, and X. L. Shan, 2013: Application of synoptic-scale anomalous winds predicted by medium-range weather forecast models on the regional heavy rainfall in China in 2010. *China Earth Sci.*, **56**, 1059–1070, doi:[10.1007/s11430-013-4586-5](https://doi.org/10.1007/s11430-013-4586-5).
- , X. L. Shan, H. Y. Liang, J. Huang, and C. H. Leung, 2014: A generalized beta-advection model to improve unusual typhoon track prediction by decomposing total flow into climatic and anomalous flows. *J. Geophys. Res.*, **119**, 1097–1117, doi:[10.1002/2013JD020902](https://doi.org/10.1002/2013JD020902).
- State Standardization Committee, 2012: Low temperature disaster of southern rice, rapeseed and orange. Rep. GB/T 27959-2011, State Standardization Committee of China, 4 pp.
- Wang, S. W., S. Q. Ma, L. Chen, Q. Wang, and J. B. Huang, 2009: *Low Temperature and Cold Disasters*. China Meteorological Press, 134 pp.
- Yan, Z. W., and C. Yang, 2000: Geographic patterns of climate extreme changes in China during 1951–1997. *Climatic Environ. Res.*, **5**, 267–272.
- Zhang, B., and Y. Li, 2013: Performance verification of medium-range forecasting by T639 and ECMWF and Japan model from June to August 2013. *Meteor. Mon.*, **39**, 1514–1520.
- Zhang, S., and B. Wang, 2008: Global summer monsoon rainy seasons. *Int. J. Climatol.*, **28**, 1563–1578, doi:[10.1002/joc.1659](https://doi.org/10.1002/joc.1659).
- Zhang, S. Y., X. N. Liu, and A. J. Sun, 1995: Climatic features of autumn low temperature damages (in Chinese). *Meteor. Mon.*, **21**, 21–24.
- Zhang, Z. J., and W. H. Qian, 2011: Identifying regional prolonged low temperature events in China. *Adv. Atmos. Sci.*, **28**, 338–351, doi:[10.1007/s00376-010-0048-6](https://doi.org/10.1007/s00376-010-0048-6).
- , and —, 2012: Precursors of regional prolonged low temperature events in China during winter-half year (in Chinese). *Chin. J. Atmos. Sci.*, **36**, 1269–1279.
- Zhao, P., P. P. Jiang, X. J. Zhou, and C. W. Zhu, 2009: Modeling impacts of East Asian ocean–land thermal contrast on spring southwesterly winds and rainfall in eastern China. *Chin. Sci. Bull.*, **54**, 4733–4741, doi:[10.1007/s11434-009-0229-9](https://doi.org/10.1007/s11434-009-0229-9).
- Zhu, C. W., X. J. Zhou, P. Zhao, L. X. Chen, and J. H. He, 2011: Onset of East Asian subtropical summer monsoon and rainy season in China. *China Earth Sci.*, **54**, 1845–1853, doi:[10.1007/s11430-011-4284-0](https://doi.org/10.1007/s11430-011-4284-0).
- Zsoter, E., 2006: Recent developments in extreme weather forecasting. *ECMWF Newsletter*, Vol. 107, ECMWF, Reading, United Kingdom, 8–17.